JOURNAL OF MATERIALS SCIENCE 31 (1996) 4213–4219

Damage propagation in carbon/silicon carbide composites during tensile tests under the SEM

A. DALMAZ, P. REYNAUD, D. ROUBY, G. FANTOZZI
Institut National des Sciences Appliquées, Groupe d'Etudes de Metallurgie Physique et de Physique des Matériaux, UMR CNRS 5510, 20, Avenue A. Einstein, F 69621 Villeurbanne cedex, France

A study has been made of the evolution of damage during monotonic and cyclic tensile tests conducted *in situ* in a scanning electron microscope on a 2.5D carbon fibre/silicon carbide matrix composite. Tests were carried out on composite specimens and the damage evolution was observed in the lateral section, using a gold square mesh deposited on the surface. Owing to the mismatch of the thermal expansion coefficients of the constituents, the initial composite already contains matrix microcracks. Cracking was observed in the transverse and longitudinal directions according to the load. This cracking consists of the growth of the pre-existing cracks, due to the thermal misfit, and the initiation of cracks in previously undamaged zones. The complex architecture, and specifically the yarn weave, induce rotation of individual fibres or bundles, which leads also to a large opening of the longitudinal cracks. Moreover, sliding at the fibre/matrix interface or at the interfaces with adjacent fibres has been pointed out, from the opening of the transverse cracks and with the help of the mesh. These mechanisms, as in other composites, could be the main origin of tensile cyclic behaviour due to a wear phenomenon in the interfacial regions.

1. Introduction

Many applications of advanced materials, such as in space shuttles, heat engines and high-speed aircraft, require strength and stability in aggressive environments at high temperature.

To overcome the high flaw sensitivity, and the lack of toughness in monolithic ceramics, fibre-reinforced ceramic matrix composites (CMCs) have been developed. The original thermomechanical properties of CMCs make them potential candidates for high-temperature structural applications. Many studies performed on CMCs have outlined the main role of damage mechanisms to control mechanical behaviour, specifically matrix microcracking and interfacial debonding which entail a non-linear and non-brittle mechanical behaviour.

The carbon fibre-reinforced silicon carbide material (C/SiC composite, manufactured and supplied by the SEP) is specified for high-temperature applications. Investigations of the tensile and fatigue behaviour of many C/SiC composites have been carried out by several authors [1–4]. However, the mechanisms of failure and the limiting load capacity for these materials is still not well understood.

In most CMCs, the failure is mainly controlled by the average and the distribution of fibre strength, and the fibre–matrix interface properties. In particular, a large effect has been noted for the interfacial shear stress associated with friction or debonding [5–8].

Hence, in this study, attention was focused on damage phenomena occurring during uniaxial tensile loading and during loading/unloading cycles of a 2.5D C/SiC composite. In particular the influence of the interfacial shear stress between the fibres and the matrix and the effect of yarn weave on the mechanical behaviour, were examined.

The aim of this present study was to observe and identify the evolution of crack growth and failure mechanisms in a 2.5D C/SiC composite under monotonic and cyclic loading, conducted *in situ* under a scanning electron microscope. These observations give a background for a better understanding and modelling of the mechanical behaviour in this kind of material.

2. Experimental procedure

2.1. Material and specimen geometry

Experiments were conducted on a 2.5D C/SiC composite manufactured and provided by the Société Européenne de Propulsion (SEP, Bordeaux, France) using a chemical vapour infiltration (CVI) process route.

The carbon fibres made up the 2.5D plain weave structure by a stack of five woven cloths. An example of the architecture is shown in Fig. 1. Initially, the fibres in the preform were coated with a thin Pyrocarbon layer giving an increased interphase in order to promote the desired pseudo-ductile behaviour in the composite. The silicon carbide matrix is formed subsequently by a chemical vapour infiltration. The as-processed composite presents a porosity fraction of

7% and a specific gravity of $2200\,kg\,m^{-3}$. The as-received material presents a large number of micro-cracks resulting from the thermal expansion mismatch between the constituents.

Monotonic and cyclic tensile tests were carried out in a SEM, and the geometry was optimized in order to obtain failure within the gauge length. Therefore, tensile specimens with a gauge section of $2 \times 4\,mm^2$ and a gauge length of 7 mm were prepared (Fig. 2).

To investigate the damage evolution in the woven structure during tensile loading, observations were made on a polished lateral surface. The plane of this lateral surface is parallel to the loading direction and perpendicular to the main plane of the weave (Fig. 2). In order to obtain more quantitative information about local displacements, a gold mesh was deposited. The mesh was produced by the following steps:

(i) deposition of a thin electrosensitive polymer (PMMA) film on the lateral surface;

(ii) electron irradiation of this film by the rastering of the SEM beam in two perpendicular directions in order to create the mesh;

(iii) dissolution of the irradiated zones and sputtering of gold;

(iv) dissolution of the remaining polymer film.

The grid produced was a periodic network of squares having 2.25 μm size and the thickness of the lines was 0.17 μm. The grid covered, on the lateral surface, an area of about $1\,mm^2$.

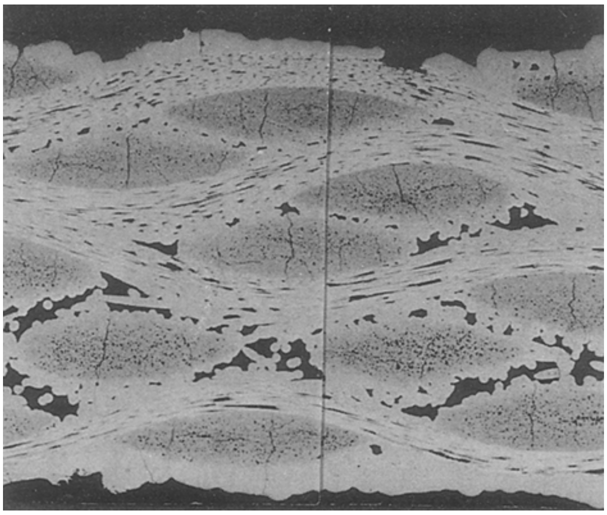

Figure 1 Polished cross-section of the as-received 2.5D C/SiC.

2.2. Test procedure

Uniaxial tension tests were carried out using an *in situ* tensile apparatus (TS 250) mounted in the SEM (Jeol 820 A). An optimized grip arrangement, adapted to the geometry of the specimen, was used. The apparatus is equipped with two sensors monitoring the load and the displacement, from which data were recorded (Fig. 3).

To investigate the influence of various parameters on the material, both monotonic and cyclic tensile tests were conducted. The observations made gave an insight into the way that microstructural damage evolves to failure in C/SiC under tension and cyclic tension/tension fatigue. Two specimens were tested: one for the monotonic tensile test and the other for the cyclic loading/unloading test. For the monotonic test, an increasing load was applied and stopped when the stress reached 70 MPa, and then applied again up to failure of the specimen. For the cyclic tests, load/unload cycles were performed with increasing maximum load of 35, 145 and 185 MPa. During the last cycle the specimen was loaded up to its failure.

3. Results and discussion

A low-magnification micrograph of the polished surface shows the woven texture of the material. The two yarn directions of the yarns within the weave are

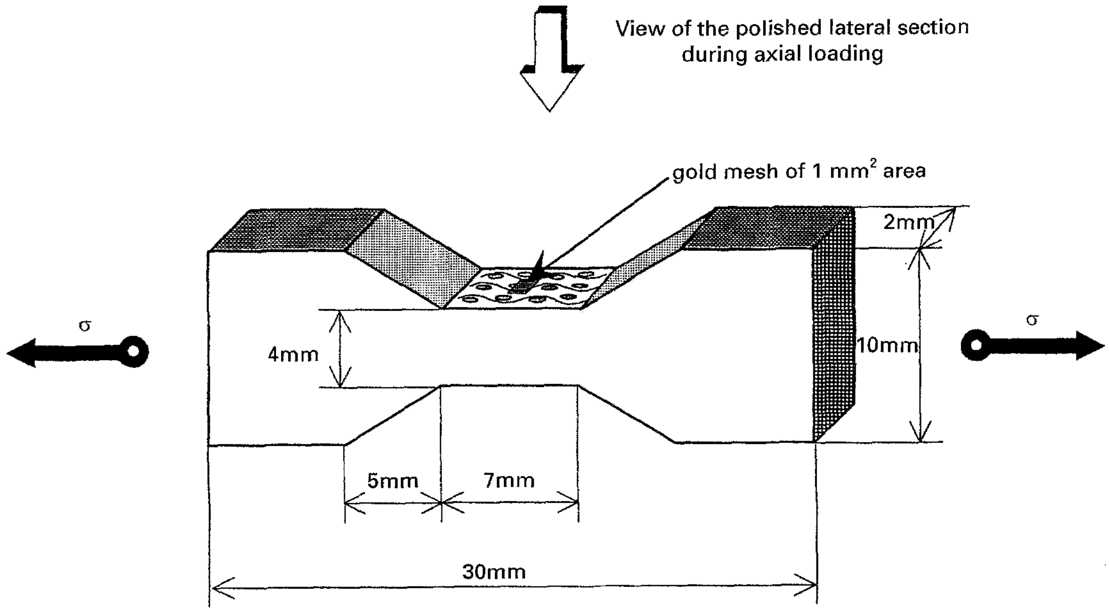

Figure 2 Specimen geometry for tensile tests under the scanning electron microscope.

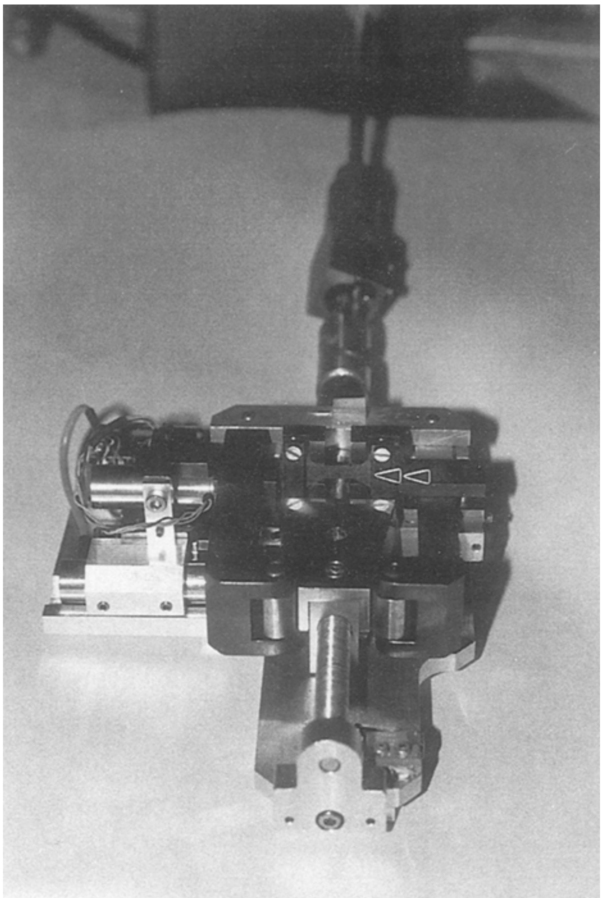

Figure 3 Tensile testing apparatus under the scanning electron microscope.

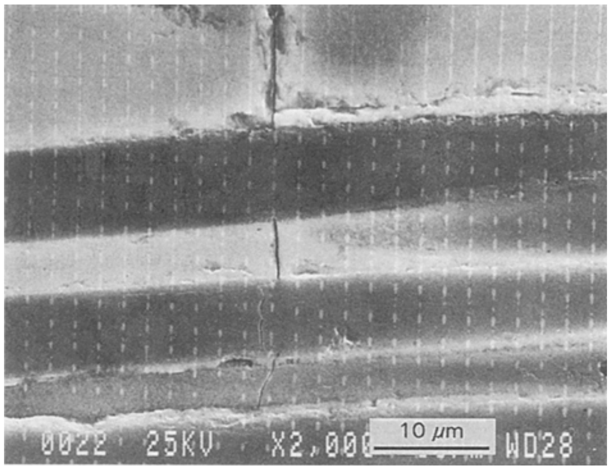

Figure 4 The mesh reveals sliding between fibre/matrix near a transverse matrix crack, $\sigma = 70$ MPa.

referred to as the warp and the weft directions with the longitudinal yarns (parallel to loading) as the weft direction. The yarns are made of fibres of 7 μm diameter; their cross-section is elliptical. The volume fraction of porosity is about 7%. Most of the porosity consists of macropores located between the fibre tows (see Fig. 1, and Figs 6 and 9 below). There is a smaller amount of cylindrical porosity inside the yarns between the fibres (see Figs 8 and 9 below).

Owing to the thermal misfit after post-process cooling, cracks exist in the as-received materials. These cracks occur mainly within the yarns, running parallel to the fibres and mostly parallel to the small axis of the ellipse (transverse cracks), as shown in Fig. 1. All the yarns (in both warp and weft directions) are cracked and exhibit, on average, 2.5 cracks per yarn (for example Fig. 1). These cracks cross the whole thickness of the yarns. There is no evidence of propagation of these cracks parallel to the fibre interface. Nevertheless, some are observed at the interface between the yarns. A few cracks are oriented parallel to the long axis of the ellipse with an average of 0.2 cracks per yarn and of 400 μm mean length. Very few cracks are initiated by the macropores as observed before loading.

3.1. Monotonic tensile tests

Monotonic tensile tests were carried out to failure of the specimen. The tensile loading was applied parallel to the fill direction, with a grip displacement rate of 15 $\mu m\, min^{-1}$. During the test, loading was stopped at a stress of 70 MPa and the damage induced was observed. The load was then applied again at the same rate until failure of the specimen occurred.

When the test was held at 70 MPa, the following features were observed.

(i) Microcracking was produced during loading in both transverse and longitudinal yarns. Cracks were developed with the transverse yarns, especially along the small axis of the ellipse. Further cracking occurs in the region surrounding the yarns at the interface between transverse and longitudinal yarns. Some of these microcracks propagated from the initial cracks in the as-received material, due to the thermal misfit between the constituents. However, there was no evidence that porosity between the yarns was at the origin of crack initiation: cracks could be created in the transverse yarn and then propagate into the porosity. These cracks ran from one fibre interface to another. It appears that the crack path can be located on the fibre surface and the pyrocarbon layer or between pyrocarbon and matrix. Our observations at high magnification covered too small an area to determine the most suitable path.

In the longitudinal yarns, microcracks, mainly located on the peripheral area of the bundle, were seen (Fig. 4). The mean distance between each microcrack was about 80 μm. For a perpendicular matrix microcrack of a peripheral longitudinal fibre, observation of the gold mesh deformation reveals sliding between fibre and matrix. By assuming a constant interfacial shear stress, τ, and by comparison of the crack opening width and the slip value for a given distance from the perpendicular crack, the interfacial sliding shear stress was found to be about 5 MPa.

(ii) Some rotation of part of a yarn was also observed; yarn cutting occurred by a perpendicular microcrack. The slight rotation of a bundle was estimated to be about 2°. For higher magnification, individual fibres on the edge of the bundles appear to rotate about 5° (Fig. 5a). In fact, the fibre yarns are not twisted in the preform, and thus, the loading on the weaves and the yarn weaving can be the most important cause of these rotations. The effects of yarn

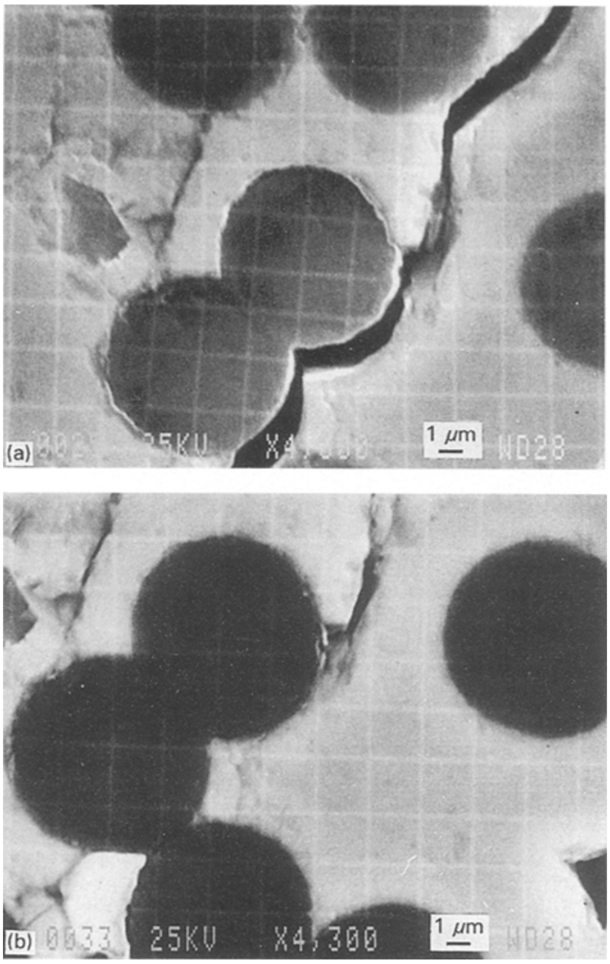

Figure 5 The gold mesh reveals the rotating movement of the peripheral fibres of the yarn. (a) $\sigma = 70$ MPa, $\theta = 5°$; (b) after failure, $\theta = 2°$. Loading direction is horizontal.

weaving have been studied by Pollock on C/C laminae [9].

Failure occurred within the gauge length at a stress level of 300 MPa and a strain of 0.9%. The fracture surface exhibits noticeable pull-out of yarns with a mean value of about 900 μm (Fig. 6a). Some transverse yarns, close to the fracture surface, have failed in their middle and have a huge transverse crack density. For the other transverse yarns, stress relaxation after failure induces a partial closure of microcracks and inverse rotation of bundles and fibres. However, residual transverse and longitudinal cracking is noted after failure, about 1.5 and 0.75 μm, respectively (Fig. 7), with a residual angle for the fibres situated on the peripheral area of the yarns of 2° (Fig. 5b).

3.2. Loading/unloading tensile test

Loading/unloading tensile tests were performed on a specimen with the same grip deformation rate as used for the monotonic tensile specimens. Loading/unloading cycles were performed with increasing maximum load 35, 145 and 185 MPa, and the specimen being observed at every step. From these investigations, the main observations made are as follows.

(i) The network of microcracks is roughly the same as in the monotonic tests. After failure, all the transverse yarns are cracked and exhibit about four transverse cracks per yarn, crossing the whole thickness. Longitudinal microcracks are roughly the same as in the as-received materials, about 0.2 cracks/yarn. The distance between the perpendicular cracks in the peripheral longitudinal fibre is about 80 μm.

(ii) Damage evolution during loading/unloading cycles has been analysed on a reduced area and is shown in Fig. 8. It appears that, for a load level of 145 MPa, the number of microcracks increases from 1 to 8 (Fig. 8a, b). At 185 MPa, the microcrack network remains unchanged, but the microcrack opening becomes wider, specifically for longitudinal cracks. After the failure of the specimen (Fig. 8c), the microcracks network is slightly varied.

Two types of crack are observed, parallel and perpendicular to the loading direction. The longitudinal cracks (i.e. in the direction of loading), evolve more rapidly with the applied stress, its opening reaching about 2.5 μm at 185 MPa, compared to 0.5 μm for the transverse cracks (Fig. 8). Longitudinal fibres appear not only at the interface between perpendicular yarns. During unloading, transverse microcracks (perpendicular to the direction of loading) close, reaching 25% of the initial opening. This phenomenon is less important for longitudinal microcracks (parallel to the load direction) because the microcracks close to about 50% of their initial opening. Thus, the behaviour of transverse cracks outlines the fact that shear lag occurs according to the classical model, the elastic behaviour of fibres being the driving force for crack closure. Moreover, longitudinal microcracks are wider and the opening less reversible during unloading than the transverse microcracks. This phenomenon is due to the absence of an undamaged elastic element in the direction perpendicular to the weave. The driving force for the opening of longitudinal matrix cracks might result from the strengthening of the yarn weave.

In addition, after unloading, the microcrack width appears to decrease with time; indeed, over 10 h the width of microcracks evolves from 0.4 μm to 0.1 μm for transverse cracking and 0.7 μm to 0.4 μm for the longitudinal one. Thus, a time-dependent behaviour has been observed.

(ii) At low magnification, rotating mechanisms, as occurring during monotonic tensile tests, were seen in the bundle, with a rotation of 1.3° (Fig. 9). Also, during unloading, the rotation of the yarn operates in the opposite sense to the initial position (0.5° unload angle).

Failure occurred at 310 MPa for 0.96% deformation in the middle of the gauge length (Fig. 6b). Like monotonic specimens, transverse yarns are cracked and some have failed in the middle. The pull-out length is about 1550 μm.

4. Conclusions

Monotonic and cyclic tensile tests have been performed in a SEM to reveal damage phenomena, such as microcrack growth and fibre/matrix interactions, occurring in a 2.5D C/SiC composite (provided

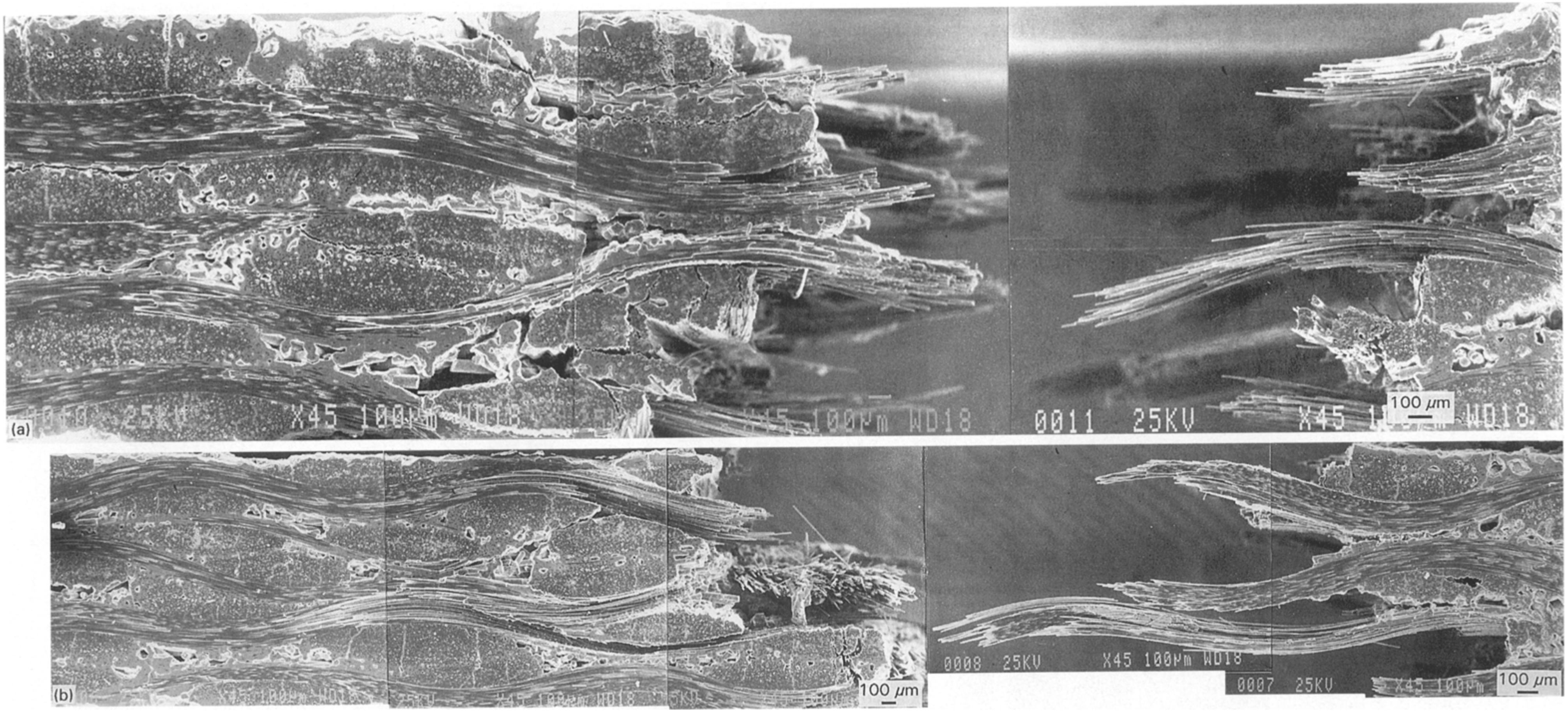

Figure 6 Overview of the 2.5D C/SiC (a) after monotonic testing at a load of $\sigma = 300$ MPa, and (b) after cyclic testing at a load of $\sigma = 310$ MPa.

by SEP). These experiments constitute a basic study for an understanding of cyclic fatigue.

From this investigation, the following conclusions can be drawn.

(i) The as-received material contains microcracks resulting from the thermal misfit after post-process cooling and a porosity of 7%.

(ii) The network of matrix microcracks evolves during both monotonic and cyclic tensile tests. Three types of crack were developed: cracking within the transverse yarns (i.e. parallel to the small axis of the ellipse), cracking perpendicular to the longitudinal yarns, and propagation of the transverse cracks in the region surrounding the transverse yarn and perpendicular to the yarn interface. A perpendicular matrix microcrack during monotonic tensile loading led to an interfacial sliding stress, τ, of 5 MPa.

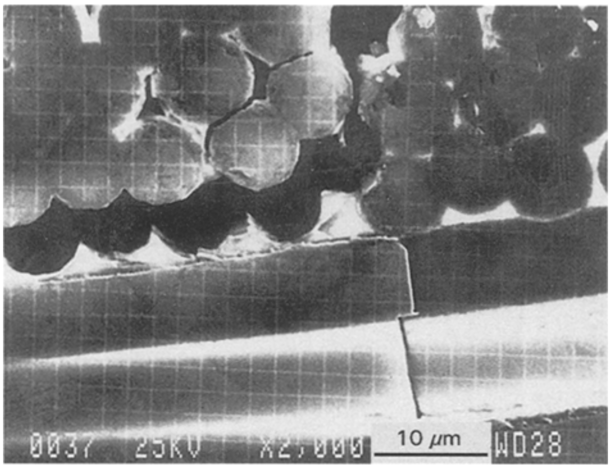

Figure 7 Residual transverse and longitudinal displacement after failure at $\sigma = 300$ MPa. Loading direction is horizontal.

During cyclic tests, wide opening of the longitudinal cracks (parallel to the loading direction) has been observed. Moreover, a time-dependent phenomenon has been detected with the observation of microcrack closure with no load applied over a few hours.

(iii) Rotation of transverse bundles and isolated fibres in the peripheral area of the yarns has been observed. This rotation might result from the strengthening of the yarns in the direction of loading.

(iv) Failure occurred at 300 MPa for 0.9% deformation for the monotonic tensile test and 310 MPa and 0.96% for the cyclic tensile test.

This behaviour is directly due to the 2.5D C/SiC composite architecture, the yarn weaving and the strengthening of the fibres in the direction of test loading.

To improve the understanding of microstructural damage evolution during monotonic and cyclic tensile tests, it is necessary to determine precisely the matrix crack density along the specimen gauge length, and the influence of the crimp angle of the woven yarns on

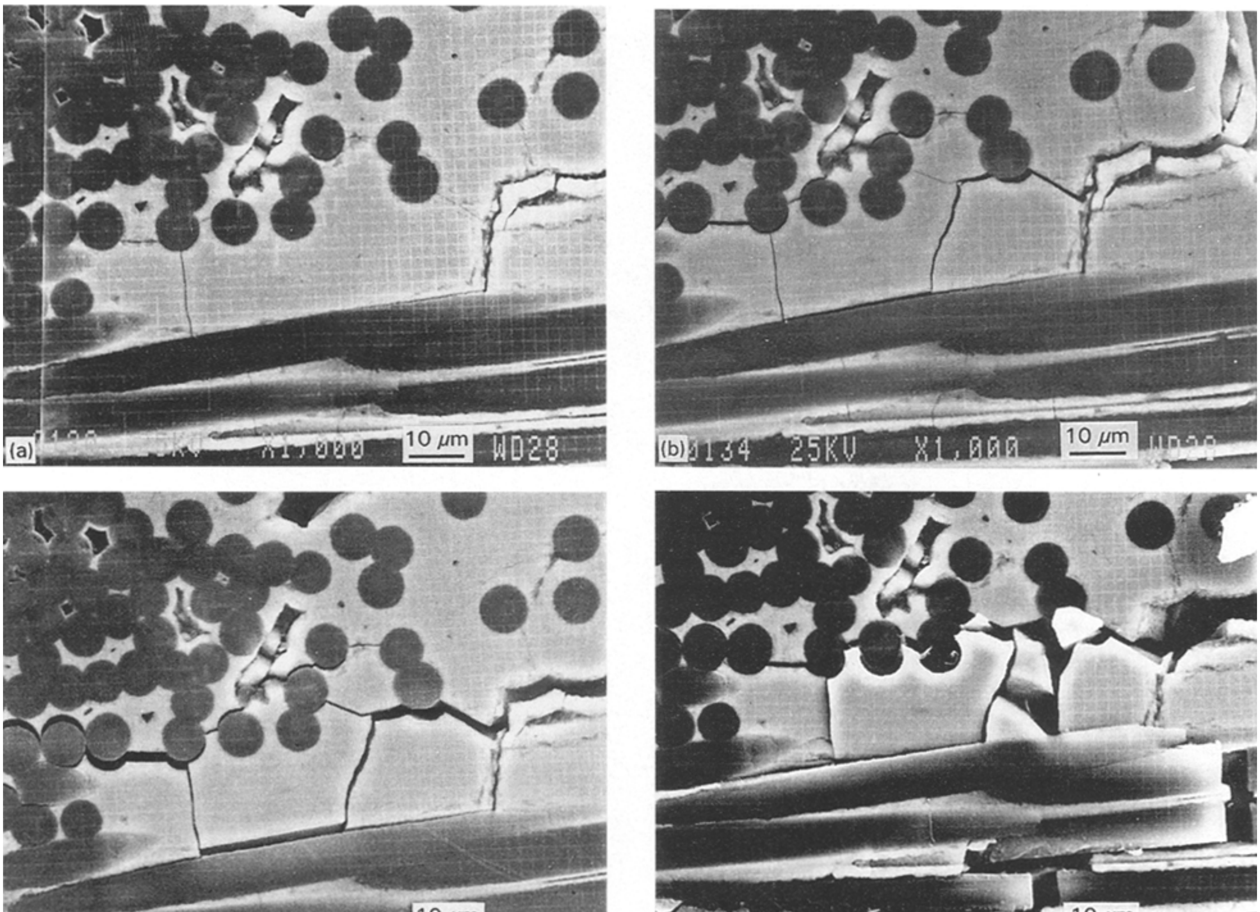

Figure 8 Damage evolution occurring during axial loading/unloading tensile tests observed in the same area: (a) $\sigma = 35$ MPa, (b) $\sigma = 145$ MPa, (c) $\sigma = 185$ MPa, (d) after failure, $\sigma_r = 310$ MPa. Loading direction is horizontal.

this density. The time-dependent phenomenon which has been highlighted must be investigated during further testing.

Acknowledgement

The authors are grateful to the SEP and to the CNRS for their interest and support in this work. The authors thank Dr M. Bourgeon, Dr F. Abbé and Dr J. Ph. Richard of SEP, for numerous fruitful discussions and for providing the materials.

References

1. F. J. ARENDTS, A. THEUER, K. MAIL and J. KUHNLE, Mechanical behavior different sized C/C-SiC tubes under multiuaxial load and temperature up to 1600 °C (1994).
2. J. W. HOLMES, "Ceramics and ceramic matrix composites", edited by S. R. Levine (ASME, New York, 1992).
3. W. L. MORRIS, B. N. COX, D. B. MARSHALL, R. V. INMAN and M. R. JAMES, *J. Am. Ceram. Soc.* **77** (1994) 792.
4. S. F. SHULER, J. W. HOLMES and X. WU, *ibid.* **76** (1994) 2327.
5. A. G. EVANS and F. W. ZOK, *J. Mater. Sci.* **29** (1994) 3857.
6. D. ROUBY and P. REYNAUD, *Compos. Sci. Technol.* **48** (1993) 109.
7. P. REYNAUD, Thèse Institut National des Sciences Appliquées (1992) ISAL 920043.
8. P. REYNAUD, D. ROUBY and G. FANTOZZI, *Scripta Metall. Mater.* **31** (1994) 1061.
9. P. B. POLLOCK, *Carbon* **28** (1990) 717.

Received 13 November 1995
and accepted 15 January 1996

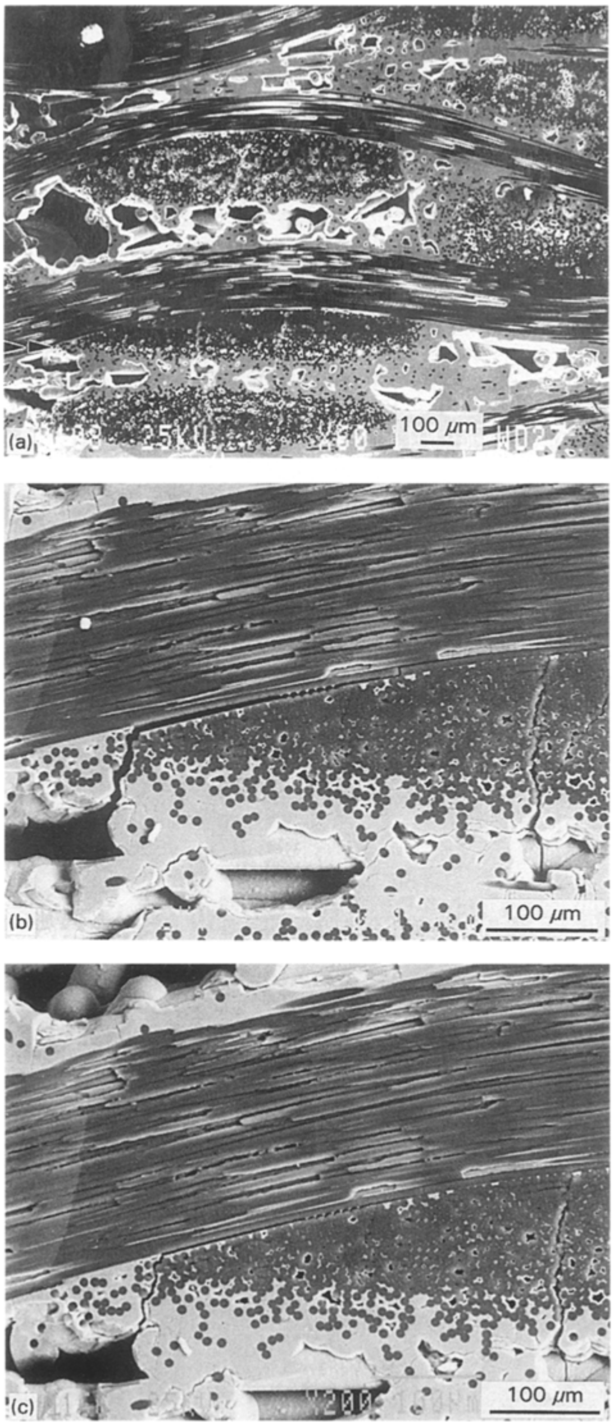

Figure 9 Rotating movement of the transverse yarns during axial loading/unloading tensile tests observed in the same area: (a) as-received composite, (b) second cycle, $\sigma = 145$ MPa, (c) second cycle, $\sigma = 0$ MPa. Loading direction is horizontal.